Common Food-Wrap Film as a Cost-Effective and Readily Available Alternative to Thermoplastic Polyurethane (TPU) Membranes for Microfluidics On-Chip Valves and Pumps

Huu Anh Minh Nguyen[1], Mark Volosov[2], Jessica Maffei[3], Roman Voronov[1,3,]*

[1] Otto H. York Department of Chemical and Materials Engineering, New Jersey Institute of Technology Newark College of Engineering, University Heights, Newark, NJ 07102, USA.

[2] Helen and John C. Hartmann Department of Electrical and Computer Engineering, Newark College of Engineering, New Jersey Institute of Technology, University Heights, Newark, NJ 07102, USA.

[3] Department of Biomedical Engineering, Newark College of Engineering, New Jersey Institute of Technology, University Heights, Newark, NJ 07102, USA.

* Corresponding author: Prof. Roman Voronov - Email: rvoronov@njit.edu

ABSTRACT: Recently, there has been an increasing effort in developing new fabrication methods for rapid prototyping of microfluidic chips using laser cutting and 3D printing. However, although these approaches can readily generate rigid parts of the devices, it is not trivial to integrate flexible components (e.g. on-chip valve and/or pump membranes) within the same build. This has led to the recent adoption of thermoplastic polyurethane (TPU) membranes sandwiched between the rigid layers to introduce the necessary flexibility to the chips. Despite its utility, TPU is not without its challenges—it is relatively expensive and surprisingly difficult to source. To overcome these difficulties, our study introduces the use of common food wrapping film as a cost-effective and readily available alternative to TPU, demonstrating its compatibility in fabricating essential microfluidic components such as on-chip valves and peristaltic pumps. Our findings show that this alternative maintains the performance standards required for sophisticated microfluidic applications while significantly alleviating logistical and financial constraints. The results show high cyclability of the membrane, up to 850,000 in continuous testing conditions, at 1 Hz, while also can block the fluid flow at as low as 250 kPa. Regarding the micropumps, it was shown that adequate flow rate of around 4 μL/min can be achieved.

Keywords: Microfluidics, rapid prototyping, 3D printing, laser cutting, on-chip valves,

integrated microvalves and micropumps, peristaltic pumps, membranes.

I. INTRODUCTION

Microfluidic devices have become pivotal in numerous scientific and industrial fields due to their ability to manipulate small volumes of fluids with high precision and efficiency. Traditionally, these devices are fabricated using techniques like photolithography, which are well-suited for creating complex, miniaturized structures. However, this method is slow, cumbersome and is prone to user error. Recent advances have expanded the microfluidics device fabrication toolkit to include laser cutting and 3D printing, enabling rapid prototyping and customization of microfluidic devices. These methods are particularly effective for constructing the rigid parts of microfluidic systems such as channels and chambers.

However, the integration of flexible components—such as membranes for on-chip valves and pumps—poses a significant challenge. These components are crucial for the dynamic control of fluid flow within the chips, necessitating materials that combine flexibility with durability. Thermoplastic polyurethane PT9200US NAT 1.0 mil (TPU) membrane from Covestro, LLC has emerged as a favored material for these applications due to its excellent mechanical properties and chemical compatibility[1-7]. However, the use of TPU is not without drawbacks. It is expensive and can be difficult to procure: specifically, the difficulty in procuring the TPU membrane from its supplier stems from several factors: Firstly, based on our communication with them, the exact specifications used in literature are not always stocked, thus requiring custom production with a limited capacity. For that reason, the company requires the customer to submit detailed technical requirements, including dimensions, application, special processing needs, and “sensitive applications” (e.g., medical, DYI) paperwork adding

further delays to the process. This hampers the widespread adoption of the technology, especially in resource-limited settings with a need for a quick turnaround, which motivated us to seek a better solution.

In response to these challenges, our study explores a simple and cost-effective alternative – the use of common food-wrap film (FWF). This material is readily-available, highly affordable, and possesses a range of physical properties that make it potentially suitable for use in microfluidic devices. To that end, here we evaluate the feasibility of using the film as a viable substitute for the TPU in the fabrication of flexible components for microfluidic devices. Specifically, we examine the performance of this material in the roles of on-chip Quake-style valves and peristaltic pumps – components fundamental to precise fluid manipulation on the microscale.

Consequently, the following experimental investigation focuses on assessing the cyclability and pressure handling capabilities of the FWF when configured as a single valve membrane. Furthermore, we also explore its effectiveness in peristaltic pump applications, measuring parameters such as flow rate and operational reliability- by quantifying the number of repeated operations of the devices in the determined conditions, specifically the performance of FWF membrane. This manuscript presents the results of these tests, providing a comprehensive evaluation of FWF against the performance benchmarks set by the TPU. Through this study, we aim to demonstrate that FWF is not only a viable alternative but also a potentially transformative product for the field of microfluidics, offering to alleviate both the logistical and the financial constraints associated with the use of exotic materials, like the TPU.

II. METHODOLOGY

II.a. Microfluidic Device Layout

The microfluidic device used for testing the FWF-based on-chip valve is illustrated in Figure 1. For simplicity, a straight channel configuration with a single valve was chosen (or three valves in the case of the peristaltic pump). The device is composed of three main layers: (1) a top control layer containing the control valve, (2) a middle flexible layer made of FWF acting as the membrane, and (3) a bottom layer containing the straight flow channel.

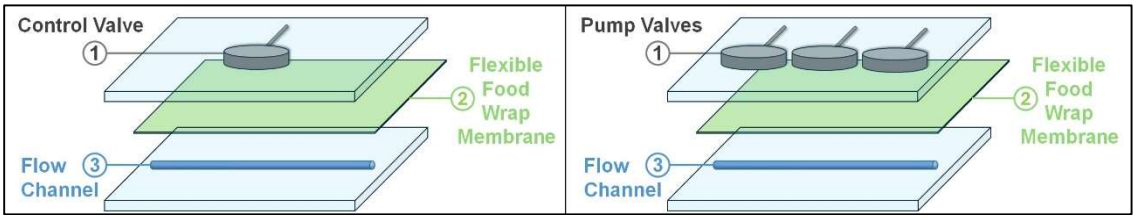

Figure 1 Layout of Microfluidic Devices with FWF Membrane for Single-Valve and Peristaltic Pump Configurations. LEFT: *The schematic on the left shows a single-valve configuration used for controlling fluid flow through a straight channel.* ***RIGHT:*** *The schematic on the right illustrates a peristaltic pump setup with three sequentially placed valves, enabling directional fluid movement through the channel. Each configuration consists of three layers: (1) the top layer containing the control or pump valves, (2) a middle layer with the flexible food wrap membrane (FWF), and (3) the bottom layer with the flow channel.*

The flow channels were designed with a semi-circular profile to enhance valve sealing performance and prevent leakage when the valve is actuated (see Figure 2). These rounded profiles were achieved through deliberate defocusing of the laser during fabrication (discussed in detail in Section II.c.). The control channels, in contrast, have a square profile and are in the top layer above the FWF membrane. This configuration forms a Quake-style valve,[8] where the combination of a semi-circular flow channel and a square control channel ensures a tight seal during operation.

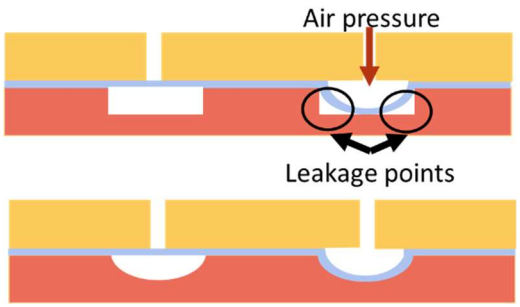

Figure 2 Illustration demonstrating why rounded-profile channels are preferred over rectangular profile ones for the fabrication of Quake-style microfluidics valves. *Specifically, an inflated membrane is unable to perfectly seal square corners of the latter, resulting in leakage. In contrast, the former results in a perfect seal.*

The device was fabricated with flow channel dimensions of 0.914 mm in width and 25.4 mm in length. The channel depth was measured to be approximately 1.2 mm. The microvalves were designed with diameters approximately 9 times the flow channel width to ensure sufficient contact area for effective sealing. For the flow and valve fatigue experiments, the control channels had dimensions of 0.178 mm in width, 0.404 mm in length, and 1.5 mm in depth, while the corresponding valve diameter was 8.61 mm. For the peristaltic pump experiments, a set of three microvalves was used, each with a diameter of 3.81 mm and depth of 1.5 mm.

These carefully designed dimensions and configurations provide an effective platform for evaluating the performance and reliability of the FWF membrane in on-chip microfluidic applications.

II.b Materials

Polymethyl methacrylate (PMMA) was used in the form of 3 mm casted clear acrylic sheets sourced from Makerstock (PA, USA). High-purity isopropyl alcohol (IPA, >99%, Sigma Aldrich, MO, USA) and chloroform (>99%, ThermoFisher, MA, USA) were employed to clean and treat the surfaces of the laser-cut acrylic slabs, respectively.

A FWF (Asahi Saran, ASIN- B0CBB9CZ82, Amazon) was used as the flexible membrane for the on-chip microvalves and micropumps. This Polyvinylidene Chloride (PVDC)-based[9] FWF is designed for baking applications and can withstand high temperatures up to 140°C. The high thermal resistance of this material was a crucial factor in its selection, as it ensures the membrane remains intact during the thermal fusion bonding process with the PMMA slabs. Non-baking FWFs were not used due to their tendency to melt under these high-temperature conditions.

II.c Laser Cutting

Microfluidic channels were fabricated in the PMMA sheets using a commercial CO_2 laser-cutting machine (Speedy 100 model, Trotec, NC, USA), equipped with a 24 × 12-inch X-Y platform, an adjustable Z-axis, and a 1.5-inch focus lens. The designs for the microfluidic geometries were created using CorelDRAW Graphics Suite X8 and then transferred to Trotec's JobControl software (version 11.4.0, Trotec, NC, USA) for laser processing. The optimal laser cutting parameters used in this study were: 35% power, 35% speed, a pulse frequency of 1000 Hz, and a single pass.

To ensure a rounded channel profile essential for the leak-free operation of on-chip Quake-style[8] microfluidic valves, the laser beam was deliberately defocused out of the normal focus plane[2]. Figure 3 show a clear progression of the rounded channel profiles depth that can be achieved via this engraving process. The final chosen depth for this study corresponded to the #3 setting shown in the image, which was obtained by placing the PMMA surface at the exact focal plane distance of the laser's 1.5-inch lens and then applying an offset Z-distance of 0.2 inches in the software to defocus the beam.

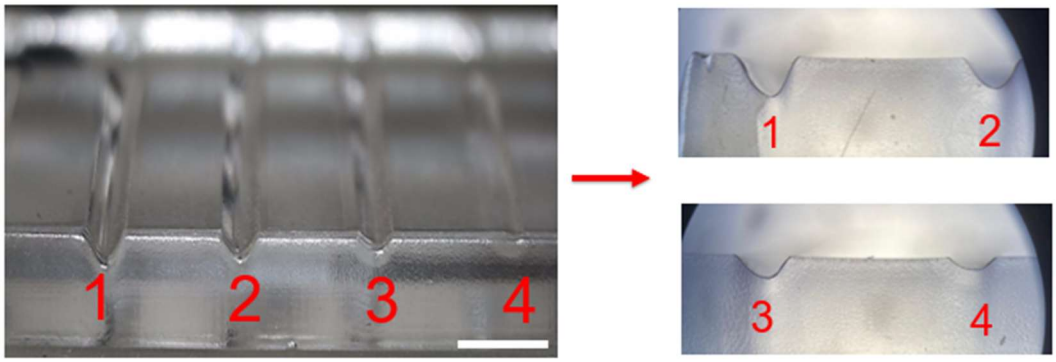

Figure 3 Rounded Profiles of Laser-Engraved Microfluidic Channels. *The semi-circular channel profiles were achieved by defocusing the laser during engraving at progressively changing distances (positions 1–4). The left pane presents a tilted view of the resulting channels, while the right pane displays a cross-sectional view of same. Scale bar: XX.*

II.d Surface Treatment of the Laser-Engraved PMMA Sheets

Following the creation of the device features, the laser-engraved PMMA sheets were cleaned by submerging and washing them twice with IPA. To smooth out rough edges and eliminate any debris generated by the high-temperature laser cutting, the surfaces were then exposed to chloroform vapor for 4 minutes. This step is crucial, as the subsequent bonding process requires smooth surfaces to ensure a strong and effective seal between the layers.

For the vapor exposure, the PMMA sheets were placed above a container filled with chloroform, ensuring that they did not come into direct contact with the liquid. This procedure was conducted at room temperature inside a fume hood to ensure safety and prevent inhalation of fumes.

II.e. Heat-press thermal bonding

A heat press equipped with dual (top and bottom) heating plates (dp-hr20t77, Dabpress, China) was used for the thermal bonding[10] of the PMMA sheets and the FWF

membrane. Achieving a high-quality seal required minimizing sample deformation, preventing leakage between layers, and ensuring a strong, irreversible bond through thermal fusion bonding. The overall process is shown in *Figure 4*.

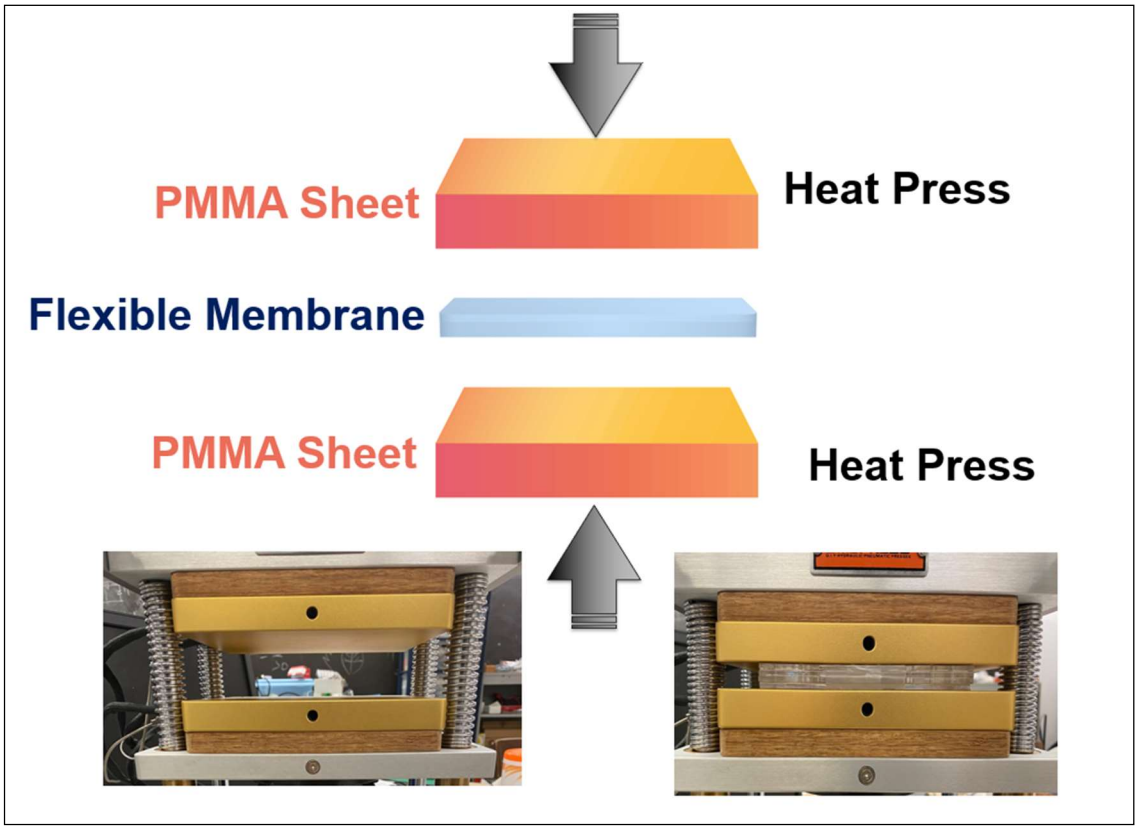

Figure 4 Schematic and Setup for Heat-Press Thermal Bonding of PMMA and Flexible Membrane. *The figure illustrates the thermal bonding process used to assemble the microfluidic device. The schematic (top) shows the sandwich structure of the PMMA sheets and flexible membrane, compressed and heated using a dual-plate heat press. The bottom images display the actual heat-press setup, highlighting the configuration of the device layers between the plates. This process ensures a strong, leak-free bond between the PMMA sheets and the flexible membrane, critical for the functionality of the microfluidic valves and channels.*

One challenge in the bonding process arises from the gas-impermeability of both PMMA and FWF, which can trap air bubbles at the PMMA/FWF interface, reducing bonding strength. To mitigate this, we incorporated laser-engraved air bubble traps in non-critical areas of the PMMA surfaces (see Figure 5C). Additionally, the PMMA substrates underwent a 2-minute plasma treatment in a plasma cleaner to enhance surface adhesion before bonding. The FWF membrane was then carefully applied and

secured using a 110 mm sewing frame (Pllieay embroidery hoops, ASIN: B093GXHSSR, Amazon) to maintain a smooth, flat, and uniform contact between the PMMA and FWF layers (see Figure 5A**)**.

Following the surface preparations, the device layers were aligned and sandwiched between two PTFE Teflon sheets (0.11 mm thick, YRYM HT, ASIN: B07H55M1ZR, Amazon) and two silicone mats (0.33" thick, Delclynee, ASIN: B093GXHSSR, Amazon) cut to fit the heating plates. These materials ensured that the chips remained in place and did not deform under the high pressure of the heat press. The aligned "sandwich" assembly (see Figure 5B**)** was subjected to a series of temperature treatments: 180°F, 200°F, 220°F, and 240°F, each applied for 10 minutes. This was followed by a gradual cooling process to room temperature (77°F), which took approximately 40 minutes, to complete the bonding.

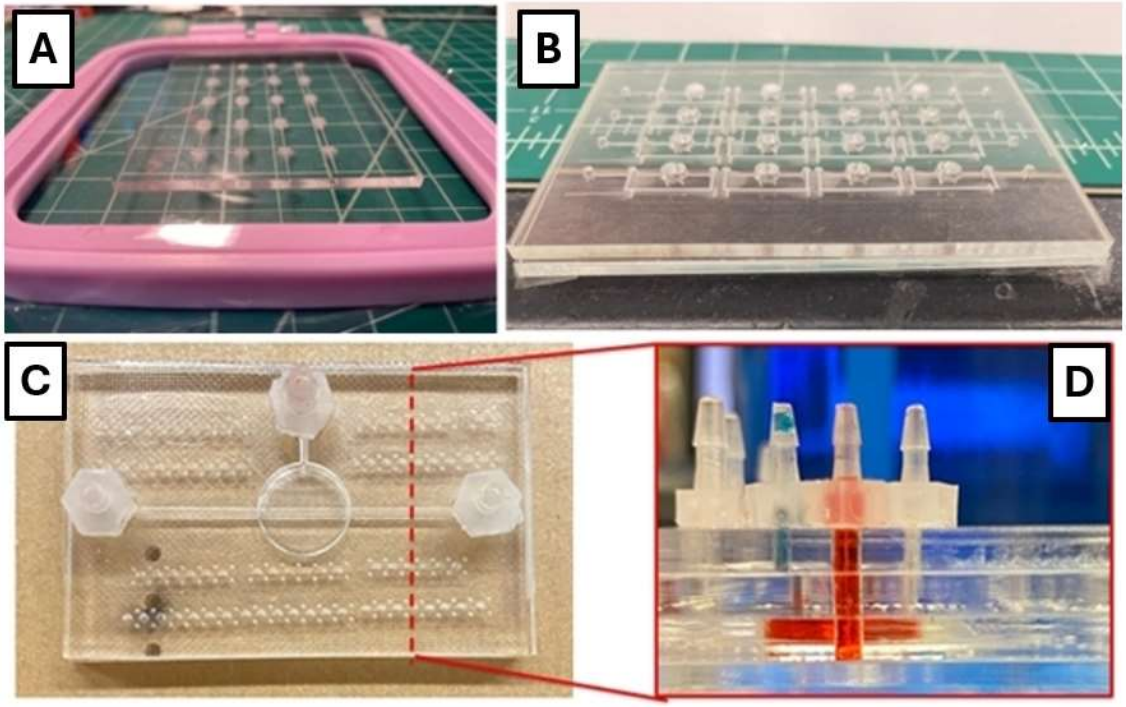

Figure 5 Fabrication and Assembly Process of the FWF-Based Microfluidic Device. *The figure illustrates key steps in the fabrication and assembly of the FWF-based microfluidic device. (A) The FWF membrane was secured in place using a 110 mm sewing frame to ensure smooth and uniform contact between the PMMA sheets and the membrane. (B) The assembled "sandwich" of PMMA sheets and FWF*

membrane prepared for the heat pressing. (C) A top view of the heat-pressed device showing the installed barbs for fluidic connections and the laser-engraved bubble traps designed to prevent air entrapment at the membrane interface. (D) A cross-sectional view of the barbs and flow channel, demonstrating red food dye-labeled fluid delivered through one of the barbs. This comprehensive assembly process highlights the fabrication techniques used to achieve reliable microfluidic functionality.

II.f. Actuation System for Microfluidic Valves and Pumps

To enable effective fluidic and pneumatic connections, barbs were bonded to the top surface of the microfluidic chips using superglue (see Figure 5 C-D). These barbs are essential components that serve as the world-to-chip interface, allowing for secure attachment to the tubing systems used for liquid and gas input/output operations.

The actuation of the fabricated microvalves and micropumps was controlled using a custom-built valve controller system[11-13]. This system employed a Wago controller (PFC100; 2 x ETHERNET; ECO, WAGO GmbH & Co. KG, Germany) to operate solenoid valves (Festo, USA), providing precise control over fluid flow and valve actuation. The entire setup was managed through a custom software interface developed in MATLAB, which automated and synchronized the operations of the microfluidic devices.

II.g. Performance Testing of the FWF Membrane Valve

The performance and durability of the FWF membrane valve were tested over a continuous period of 10 days, operating at a frequency of 1 Hz. Every thousand cycles, the valves were subjected to functional testing to assess their ability to stop fluid flow without any leakage. A colored liquid, created by mixing water and red food dye, was used to easily visualize the fluid flow within the channels.

For all tests, the input pressure was maintained at 5 psi, while the valve actuation pressure was fixed at 50 psi to ensure consistent testing conditions.

Visualization of fluid flow and valve functionality was performed using a Microqubic 3D MRCL700 microscope (CN Tech, Wisbech, England), with transmitted (brightfield) light source, and the stock "medium zoom" lens from the manufacturer.

III. RESULTS AND DISCUSSION

III.a. Baseline Flow Rate Characterization in a Heat-Bonded PMMA-FWF Straight Channel Device

To establish a reference for the performance of more complex microfluidic devices, we first characterized the simplest device configuration: a straight channel. This experiment was designed to evaluate the flow rate as a function of input pressure in a device assembled by heat bonding PMMA slabs with a food-wrap film (FWF) membrane sandwiched between the layers (see Figure 6). The results from this baseline experiment provide key performance metrics that can be compared with future microfluidic designs involving more complex geometries and functional components.

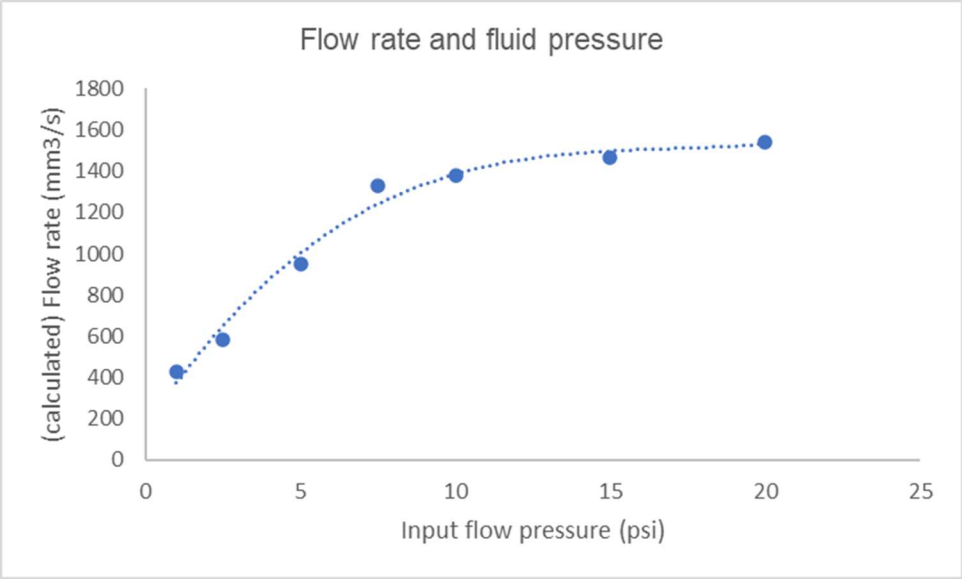

Figure 6 Flow Rate as a Function of Input Flow Pressure for a Baseline Straight Channel Microfluidic Device Prepared via Heat-Bonding PMMA and FWF Layers. *Flow rate is calculated by measuring the volume of the liquid collected at the device's outlet and dividing it over the time that it took to collect the volume.*

Specifically, Figure 6 illustrates the relationship between input pressure and the resulting flow rate to assess the straight channel's performance under varying pressure conditions. The flow rate was determined using the volumetric displacement of fluid over time across different input pressures. As shown, the flow rate increases almost linearly between 1 and 10 psi, from approximately 400 mm^3/s to 1,400 mm^3/s. After the 10-psi mark, the flow rate plateaued at around 1,500 mm^3/s. This trend is characteristic of straight channels, where flow resistance decreases with increasing pressure, but eventually levels off at higher pressures. This plateau suggests that the channel approaches its maximum capacity for fluid transport under the given pressure conditions. These results establish key operational parameters for the straight channel microfluidic device, assembled by heat bonding PMMA slabs with the FWF membrane, and serve as a performance benchmark for more complex designs.

III.b. Determination of Closing Pressure for the FWF Valve via Leakage Characterization

To evaluate the effectiveness of the valve seal in our microfluidic device, we measured the leakage as a function of input pressure applied to the valve's control channel. As the air pressure is increased in the control channel, we expect the valve to create a tighter seal, reducing the leakage flow rate until complete closure is achieved. This test is critical in determining the pressure threshold required for effective valve operation, as well as understanding any limitations in sealing performance. By plotting the flow rate at the device outlet against the input pressure, we can visualize the leakage behavior across a range of pressures (see Figure 7).

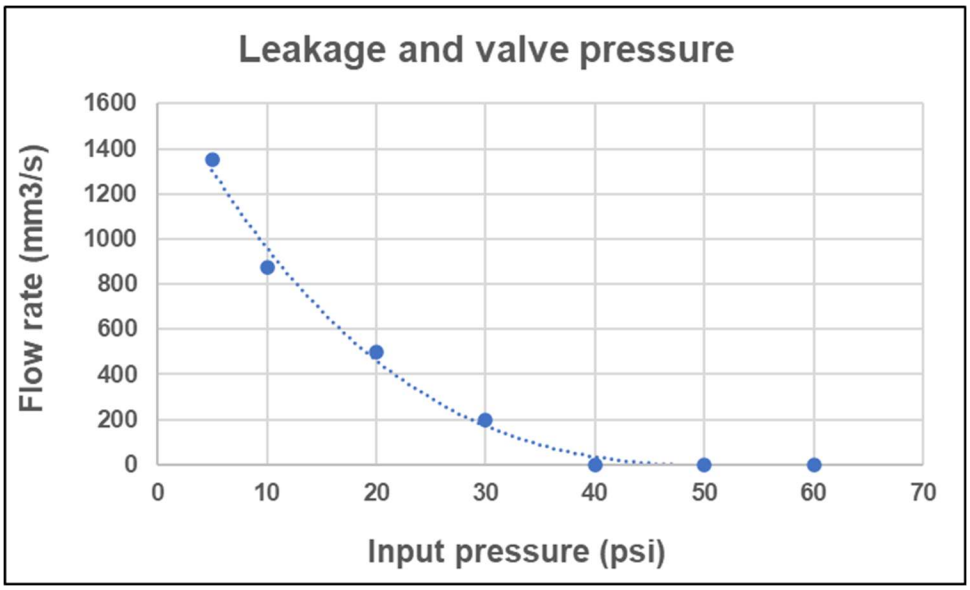

Figure 7 Leakage Flow Rate as a Function of FWF Valve Control Pressure. The graph depicts how the leakage flow rate decreases with increasing input pressure applied to the FWF valve's control channel. The flow rate drops sharply between 0 and 40 psi, indicating improved valve sealing, and approaches zero around 50 psi, demonstrating effective closure of the valve.

As shown in Figure 7, the leakage flow rate decreases exponentially as the input pressure increases. Between 0 and 40 psi, the flow rate drops significantly, from 1,400 mm^3/s at 0 psi to < 200 mm^3/s at 40 psi. Beyond 40 psi, the leakage flow rate

approaches zero, indicating that the valve has effectively sealed. These results suggest that the valve requires a minimum of 50 psi to achieve full closure and prevent leakage, providing an operational benchmark for pressure-driven valve control in this system.

For comparison, this required pressure is significantly higher than the ~30 psi needed to fully close a similar valve made out of poly(dimethyl siloxane) (PDMS) – the gold standard material for microfluidics device fabrication [14]. A likely explanation is that PVDC, the primary component of the FWF, has a Young's modulus that is 3-6 times higher than that of the PDMS, specifically in the range of 300-550 MPa for PVDC vs 1.32 to 2.97 MPa for PDMS [15].

This marked difference in mechanical properties likely explains why a higher pressure is needed to achieve complete valve closure when using the FWF membrane. Nevertheless, the FWF's sealing mechanism under high pressure is robust, achieving a tight and impermeable seal. The optimization of the device's channel dimensions and laser engraving process further ensures reliable valve function, which is crucial for precise fluid control in future applications.

III.c. Durability and Burst Pressure of the FWF-Based Microvalves

The durability and reliability of microvalves in microfluidic systems are critical factors in determining their practical utility. In this study, we performed extensive testing to evaluate the performance of our microvalves under repeated cycling conditions. Our results indicate that after approximately 400,000 cycles, the microvalves began to show signs of leakage, which, although minor at first, signaled gradual deterioration of the FWF membrane's integrity with extended use. As the

cycling continued, the severity of leakage increased, eventually compromising valve functionality.

Figure 8A visually presents the leakage after several cycles, showing minimal or negligible differences in fluid leakage levels. This suggests that after 400,000 cycles, the leakage remains stable and does not significantly worsen until the membrane physically fails, marked by the presence of dye within the valve layer (see Figure 8B). Complete valve failure occurred after approximately 850,000 cycles, at which point the microvalves ceased to function and were no longer suitable for further experimentation or practical applications.

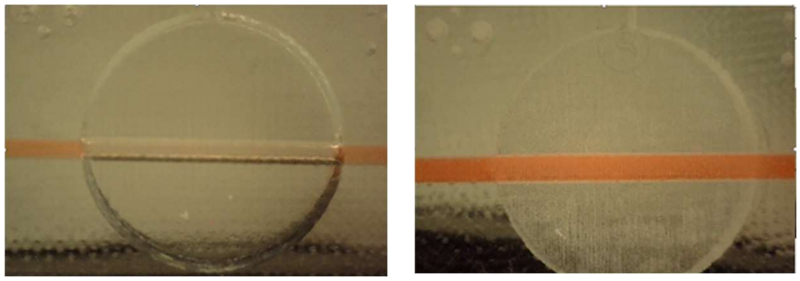

Figure 8 *(A) Close-up images of non-leak valves after ~400k cycles, and (B) leaked valves after ~850k cycles.*

Additionally, we conducted burst pressure testing to determine the maximum pressure the FWF valves could withstand. The devices, assembled by thermal bonding of acrylic and FWF layers, were tested under the highest achievable lab pressure of 60 psi. Even at this maximum pressure, there were no signs of leakage or device failure. These findings demonstrate that the thermal bonding method used establishes a robust bond between acrylic and FWF, making it a reliable process for practical applications and large-scale production.

III.d. Application of FWF Membrane Valves: On-Chip Peristaltic Pumping System

In addition to its use as a membrane for Quake-style microvalves, the FWF can also be utilized in micro-pumps, employing a peristaltic mechanism to pump fluids

without the need for external pumps. In this setup, three pumps of identical size were placed next to each other (**Error! Reference source not found.**) and programmed to open and close in sequence, thereby pushing the fluid through the channel.

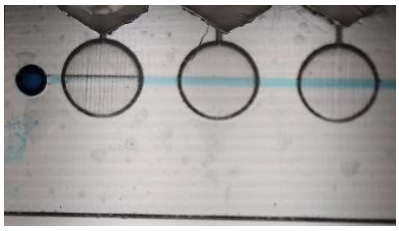

Figure 9 Characterization of on-chip peristaltic micro-pumps utilizing the FWF membrane valve.

The 3-pump system, operating at the fasted frequency of 1 Hz, generated a flow rate of 1.33 µL/min, measured by the volume of collected fluid and operation time. The system demonstrated continuous operation without failure within the 400,000 cycles expected lifetime of the FWF membrane and efficiently pushed fluid through the channels at a consistent pace. This successful demonstration of the pump system highlights the feasibility of FWF-based membrane valves for use in peristaltic, on-chip micro-pumps. These pumps can be seamlessly integrated into microfluidic systems for a variety of applications.

IV. CONCLUSIONS

This study demonstrates the viability of food-wrap film (FWF) as a cost-effective and readily available alternative to thermoplastic polyurethane (TPU) membranes in microfluidic devices, particularly for on-chip valves and pumps. The findings highlight the suitability of FWF for microfluidic applications due to its affordability, accessibility, and ease of integration into existing fabrication workflows.

FWF exhibited performance metrics comparable to TPU, including reliable sealing capabilities with a closing pressure as low as 250 kPa and robust flow rates of approximately 4 µL/min in peristaltic pump configurations. Durability tests showed that the FWF membrane could withstand up to 850,000 actuation cycles under continuous operation at 1 Hz, indicating its mechanical stability and suitability for long-term applications. Additionally, the high thermal resistance of FWF (up to 140°C) enables integration into PMMA-based devices through thermal bonding without risk of melting or deformation during fabrication. The straightforward fabrication process further underscores the potential for large-scale production of FWF-based microfluidic devices.

The combination of FWF's low cost, mechanical robustness, and ease of implementation highlights its broad applicability in microfluidic systems, particularly in resource-limited settings and disposable diagnostic applications. Future work should focus on optimizing the design and operation of FWF-based devices, exploring advanced geometries, pump configurations, and operation parameters to enhance performance and expand the scope of its application in microfluidics.

V. ACKNOWLEDGMENTS

Funding: This work was supported by the National Institutes of Health (NIH) grant number 1R15GM145610-01, the National Science Foundation (NSF) Award Number 2141029 and the New Jersey Health Foundation (Foundation for Health Advancement, Inc.) Innovation Grant Award Number IFHA 10-22.

CRediT Author Statement

Roman Voronov: Conceptualization, Methodology, Validation, Resources, Writing-Review and editing, Supervision, Project Administration, Funding acquisition Minh Nguyen: Conceptualization, Methodology, Formal Analysis, Investigation Writing-Original draft preparation, Data curation, Visualization. Mark Volosov: Software, Data curation. Jessica Maffei: Methodology.

Tables and Table Captions

Table 1

Figure Captions:

Figure 10

Figures

References

(1) Fan, Y.; Huang, L.; Cui, R.; Zhou, X.; Zhang, Y. Thermoplastic polyurethane-based flexible multilayer microfluidic devices. *Journal of Micro/Nanolithography, MEMS, and MOEMS* **2020**, *19* (2), 024501-024501.
(2) Shaegh, S. A. M.; Pourmand, A.; Nabavinia, M.; Avci, H.; Tamayol, A.; Mostafalu, P.; Ghavifekr, H. B.; Aghdam, E. N.; Dokmeci, M. R.; Khademhosseini, A. Rapid prototyping of whole-thermoplastic microfluidics with built-in microvalves using laser ablation and thermal fusion bonding. *Sensors and Actuators B: Chemical* **2018**, *255*, 100-109.
(3) Ameri, A. R.; Imanparast, A.; Passandideh-Fard, M.; Shaegh, S. A. M. A whole-thermoplastic microfluidic chip with integrated on-chip micropump, bioreactor and oxygenator for cell culture applications. *Analytica Chimica Acta* **2022**, *1221*, 340093.
(4) Shaegh, S. A. M.; Wang, Z.; Ng, S. H.; Wu, R.; Nguyen, H. T.; Chan, L. C. Z.; Toh, A. G. G.; Wang, Z. Plug-and-play microvalve and micropump for rapid integration with microfluidic chips. *Microfluidics and Nanofluidics* **2015**, *19*, 557-564.
(5) Pourmand, A.; Shaegh, S. A. M.; Ghavifekr, H. B.; Aghdam, E. N.; Dokmeci, M. R.; Khademhosseini, A.; Zhang, Y. S. Fabrication of whole-thermoplastic normally closed microvalve, micro check valve, and micropump. *Sensors and Actuators B: Chemical* **2018**, *262*, 625-636.
(6) Khaksari, S.; Ameri, A. R.; Taghdisi, S. M.; Sabet, M.; Bami, S. M. J. G.; Abnous, K.; Shaegh, S. A. M. A microfluidic electrochemical aptasensor for highly sensitive and selective detection of A549 cells as integrin α6β4-containing cell model via IDA aptamers. *Talanta* **2023**, *252*, 123781.
(7) Banejad, A.; Passandideh-Fard, M.; Niknam, H.; Hosseini, M. J. M.; Shaegh, S. A. M. Design, fabrication and experimental characterization of whole-thermoplastic microvalves and micropumps having micromilled liquid channels of rectangular and half-elliptical cross-sections. *Sensors and Actuators A: Physical* **2020**, *301*, 111713.
(8) Melin, J.; Quake, S. R. Microfluidic large-scale integration: the evolution of design rules for biological automation. *Annu. Rev. Biophys. Biomol. Struct.* **2007**, *36* (1), 213-231.
(9) Wrap, A. *Asahi Wrap (TM) food wrap, ASAHI KASEI*. ASAHI KASEI Home Products Corperation, 2024. https://www.asahi-kasei.co.jp/saran/global/asahiwrap/english/ (accessed October 3, 2024).
(10) Zhu, X.; Liu, G.; Guo, Y.; Tian, Y. Study of PMMA thermal bonding. *Microsystem Technologies* **2007**, *13*, 403-407.
(11) Nguyen, M.; Tong, A.; Volosov, M.; Madhavarapu, S.; Freeman, J.; Voronov, R. Addressable microfluidics technology for non-sacrificial analysis of biomaterial implants in vivo. *Biomicrofluidics* **2023**, *17* (2).
(12) Tong, A.; Pham, Q. L.; Shah, V.; Naik, A.; Abatemarco, P.; Voronov, R. Automated addressable microfluidic device for minimally disruptive manipulation of cells and fluids within living cultures. *ACS Biomaterials Science & Engineering* **2020**, *6* (3), 1809-1820.

(13) White, J. A.; Streets, A. M. Controller for microfluidic large-scale integration. *HardwareX* **2018**, *3*, 135-145.
(14) Mohan, R.; Schudel, B. R.; Desai, A. V.; Yearsley, J. D.; Apblett, C. A.; Kenis, P. J. Design considerations for elastomeric normally closed microfluidic valves. *Sensors and Actuators B: Chemical* **2011**, *160* (1), 1216-1223.
(15) Ariati, R.; Sales, F.; Souza, A.; Lima, R. A.; Ribeiro, J. Polydimethylsiloxane composites characterization and its applications: a review. *Polymers* **2021**, *13* (23), 4258.